Boosting Perovskite Solar Cell Efficiency Using Tin Based Compounds

Chinaecherem Tochukwu Arum [a*], Simon Bbumba [b,c,d *], Moses Kigozi [e], Ibrahim Karume [b], Muhammad Jawad [f], Ivan Kiganda [b], Hussein Kisiki Nsamba [b], John Ssekatawa [b] and Muhammad Ntale [b]

[a] *Department of Material Science and Explosives, Faculty of Science, Nigerian Defence Academy, PMB 2109, Kaduna, Nigeria.*
[b] *Department of Chemistry, College of Natural Sciences, Makerere University, P.O. Box-7062, Kampala, Uganda.*
[c] *Department of Science, Faculty of Science and Computing, Ndejje University, P.O. Box 7088, Kampala, Uganda.*
[d] *Department of Chemistry, Faculty of Science, Muni University, P.O. Box- 725, Arua, Uganda.*
[e] *Department of Chemistry, Busitema University, P. O. Box -236, Tororo, Uganda.*
[f] *Department of Environmental Chemistry, Faculty of Science, Nigerian Defence Academy, PMB- 2109, Kaduna, Nigeria.*

Authors' contributions

This work was carried out in collaboration among all authors. Authors CTA, SB, MK, IK, MJ, IK, HKN, JS and MN participated in writing the main manuscript and discussed the previous findings. All authors read and approved the final manuscript.

Review Article

_____

*Corresponding author: Email: sbbumba@ndejjeuniversity.ac.ug; arumtochi7@gmail.com;

ABSTRACT

Herein, we reviewed lead (Pb) free perovskite solar cells (PSCs) using Tin (Sn) compounds (FASnI$_3$, CsSnI$_3$) as alternative materials that are stable, cheap, and environmentally benign. These devices have an efficiency of 13 %, but when compared to the 25.7 % of Pb, it is still low. Oxidation of Sn^{2+} to Sn^{4+}, surface defects, and low energy band gap alignment are concerns for the application Sn since they lower the device performance. It is worth mentioning that several solutions have been implemented to address the drawbacks, such as the use of encapsulation technology, the preparation method, and charge carrier materials. In this regard, encapsulation technology is applied to reduce aerial oxidation, which results in high stability. Furthermore, the charge carrier materials play a crucial role in energy band alignment, reduction in hole and electron recombination, and improvement of the contact between the interfacial surfaces. In brief, this review summarizes the Sn-based perovskites solar cells and how their efficiency can be modified based on the preparation method, use of either the solvent or the anti-solvent, charge transport materials, and encapsulation technology.

1. INTRODUCTION

For renewable energy sources, high-efficiency solar cell technologies like perovskite materials are being investigated. However, worries about lead toxicity in conventional formulations have prompted the creation of lead-free substitutes, such as tin-based perovskites, which salvage health and environmental issues while maintaining great performance [1,2].

Metal-halide-perovskite-based photovoltaics have shown remarkable advancements in solar cell performance over a very short span of about ten (10) years. These advancements have surpassed those achieved by other main photovoltaic semiconductor materials, such as organic, cadmium telluride, and copper indium gallium selenide. The present emphasis is on the commercialization of perovskite solar cell technology and the challenges faced in achieving and maintaining high efficiency, stability, and eco-friendliness in the photovoltaic field [3].

Research on modern photovoltaic devices has yielded various photovoltaic concepts utilizing different light-absorbing materials, including semiconducting inorganic compositions such as copper indium gallium selenide (CIGS), CdTe, quantum dots, organic semiconductors, and dyes. These advancements have been made since the invention of crystalline silicon solar cells in the 1950s [4] and have been documented by [5]. However, solar cells using these novel principles have faced several obstacles in surpassing the efficiency (26.7 %) previously achieved by silicon materials. Around ten years ago, metal halide perovskites (MHPs) of APbI$_3$ (ABX$_3$ type) were discovered as potential materials for absorbing light in light-harvesting applications [6–8]. Metamaterials have exceptional characteristics in the fields of photovoltaics [9] and optoelectronics[10]. Moreover, they have significant commercial prospects because of their substantial capacity for expanded, extensive vacuum-free production [11]. Furthermore, since the initial publication on perovskite solar cells (PSCs) in 2009, significant advancements have been made, resulting in a remarkable enhancement in their power conversion efficiency (PCE) from around 3 to 25.7% [6–8,12,13]. In only ten years, this advancement reached a remarkable efficiency of 25 %, surpassing that of crystalline silicon solar cells [4].

Perovskites with the ABX$_3$ formula have a straightforward cubic structure. This structure is made up of eight BX6^{4-} octahedral sublattices that share corners and provide a center space for the A-site. In this formula, A and B represent cations, while X represents a halide anion [14]. Typically, the A-site is filled with either a Cs inorganic cation or organic molecules such as CH$_3$NH^{3+} (MA$^+$) and NH$_2$CHNH^{2+} (FA$^+$). In addition, the B-site is predominantly filled with metal cations of Pb^{2+} or Sn^{2+} from group IV-A, whereas X usually represents Cl$^-$, Br$^-$, or I$^-$. MHPs, or metal halide perovskites, are a kind of ionic crystals that have a soft nature. They can tolerate defects, which makes their synthesis straightforward and contributes to the development of highly efficient solar systems [15]. Nevertheless, PeSCs may also induce ion migration inside the lattice, hence diminishing operational dependability and limiting the

commercial use of PeSCs [16,17]. Therefore, various techniques have been used to address these problems by modifying either the A-site or X-site and adding controls, resulting in improved efficiency and operational stability [16–19].

Following the successful development of PSCs with an efficiency of over 25 % at the cell scale, the subsequent phase of research driven by commercial interests is mostly centered on investigating the stability of PSCs when exposed to continuous light-soaking conditions. This study is particularly concerned with the large-area submodules scale and has been documented by [16,17]. In order to be successfully brought to market, PSCs must be able to endure both light and thermal pressures throughout their operating lifespan. Therefore, it is crucial to focus research on the light stability of PSCs. Nevertheless, these studies have significant constraints, impeding the commercialization of PSCs. Conversely, the investigation of PSCs' response to light, heat, or humidity in terms of their thermal behavior and structural stability is a rapidly expanding field of research [18,19].

1.1 Pb in PSCs and Its Effect on the Environment

The crystal structure of Pb-based perovskites can be represented by the chemical formula ABX_3. In this formula, the A-site consists of large organic cations such as $CH_3NH_3^+$ (MA), $[(NH_2)_2CH]^+$ (FA), or inorganic Cs^+. The B component can be lead (Pb^{2+}), Sn^{2+}, or other divalent metal cations. The X component is a halide anion, such as I^-, Br^-, or Cl^-. The best-performance PSCs presently use Pb and organic A cations[13]. Pb-based PSCs undergo decomposition when exposed to moisture, UV radiation, oxygen, high temperature, or a combination of these elements. The decomposition process yields PbI_2 or $PbBr_2$, a small quantity of metallic Pb, and carbonated components that eventually transform into hydroiodic acid (HI) and methylamine or formamidinium [20]. PbI_2 and $PbBr_2$ exhibit moderate solubility in water, with a solubility product on the order of 10^{-8}. This solubility is significantly higher compared to other heavy metal compounds, such as CdTe, which has a solubility product of less than 10^{-34} [21].

2. TIN-BASED PEROVSKITES

Several works have concentrated on tin-based PSCs after the research conducted by [22,23], which achieved an efficiency of about 6 %. Recent advancements in Sn-based PSCs have shown significant improvements in performance, achieving a power conversion efficiency (PCE) of more than 14 % [24-26].

Nevertheless, Sn-based PSCs often demonstrate elevated short-circuit current densities ranging from 20 to 25 mA cm^{-2} owing to their small bandgaps. It is worth noting that the solar cells have an average open-circuit voltage (V_{OC}) of roughly 0.5 V, which is much lower than the 1.1 V of the Pb-based perovskites. The biased and unwanted oxidation of Sn^{2+} to Sn^{4+} results in the materials being heavily doped with p-type impurities, which act as p-type dopants in the structure and result in a significant increase in photocarrier recombination and an unacceptably high concentration of dark carriers. Considerable work has been devoted to improving the performance and stability of tin-based PSCs, as shown by the studies conducted by [28–30].
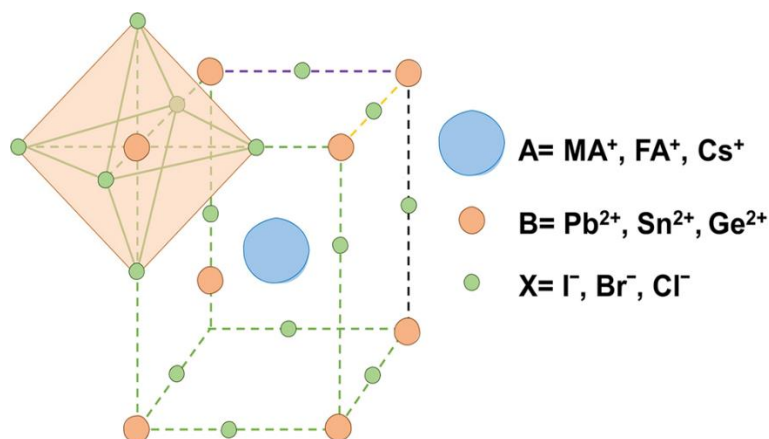

Fig. 1. Schematic representation of a perovskite material [27]

Among the several types of perovskites, the presence of Pb^{2+} is still necessary to provide outstanding photoelectric characteristics. Nevertheless, the byproducts of lead-based perovskites may have harmful effects on the environment, as well as on people and other organisms. These pose a barrier to the widespread use of this technology [31]. Consequently, there has been a recent surge of interest in lead-free perovskite light absorbers that are less harmful. Tin is seen as a less dangerous substitute for lead since it belongs to the same group 14 (IVA) of the periodic table as lead. In addition, tin-based perovskites have optical bandgaps that span between 1.2–1.4 eV, as reported by [32]. This range is in close proximity to the ideal bandgap of 1.34 eV for the Shockley–Queisser (SQ) limit, as defined by Shockley and Queisser in 1961, under the AM 1.5 solar spectrum. Therefore, it is anticipated that tin-based perovskites would have favorable uses in photovoltaic and other optoelectronic devices. The use of tin-based halide perovskites as conducting channels for thin-film field-effect transistors was first presented almost two decades ago [33,34].

In 2012, researchers used a tin-based perovskite as a light absorber in Schottky solar cells, resulting in a remarkable PCE of 0.9 % [35]. In 2014, both Noel et al. and Hao et al. independently published their findings on tin-based perovskite solar cells (PSCs) around the same time. They achieved a promising PCE of about 6% [22,23]. These first findings have sparked enthusiasm among researchers, and tin-based PSCs have made significant advancements in recent years. As an example, tin-based PSCs with modest dimensions have achieved a PCE above 9%, according to [36]. The primary issue faced by tin-based PSCs is their limited air stability, which arises from the susceptibility of Sn^{2+} to oxidation, resulting in the formation of Sn^{4+} [37]. Therefore, several methods have been devised to prevent the oxidation of tin-based perovskites throughout the manufacturing and use of devices. In recent times, a number of innovative strategies have been created, resulting in a significant improvement in the efficiency of tin-based PSCs. At now, tin-based PSCs exhibit a peak power conversion efficiency (PCE) above 13 % and possess exceptional device stability. This makes them a very appealing photovoltaic technology that warrants continued development in the next years. At the outset of this paper, we provide an overview of the characteristics of tin-based perovskites, including their fundamental properties and the construction of photovoltaic devices known as PSCs. The study conducted by [7] discusses the use of compositional engineering as a simple method to improve the performance of perovskite-based solar cells. The emphasis is on how the characteristics of these cells may be enhanced by modifying the crystal structures and the types of cations/anions present, specifically in tin-based perovskite solar cells. Sn-Pb mixed perovskite materials have an expanded absorption range in the near-infrared (NIR) region and have significant potential for use in tandem solar cells (Liao et al., 2017; Zhao et al., 2017).

3. PREPARATION METHODS OF SN HALIDE PEROVSKITE FILMS

Prior to the characteristics of the Sn halide perovskite films and devices, preparation procedures are necessary Yokoyama et al., 2016; Y. Yu et al., 2016). The selection of a process often relies on its compatibility with the chemical composition of the material and the characteristics of the final product. The thin films are typically fabricated using solution processing, specifically using the spin-coating approach, which may be customized according to specific requirements [23,41–44]. In addition to spin-coating, alternative techniques such as thermal evaporation [39,45,46], vapor-assisted deposition [40,47], and solvothermal process [48] have been documented.

3.1 Solution Process

The solution technique has been extensively used in the fabrication of Sn halide perovskite materials and devices. This technology is both cost-effective and quickly processed, and it may be adjusted to provide highly useful layers in devices. In addition, it enables the fine-tuning of film thickness, annealing temperature, and composition, as demonstrated by [42] in their creation of a compact and uniform thin film of $MASn0.5Pb0.5I_3$. By incorporating 50 % Pb into the chemical composition of the compound, they were able to achieve a continuous and uniform film morphology, which was not possible with the Sn-only perovskite film. The influence of film shape on the characteristics and performance of perovskite materials and devices is unquestionable [23,40,49]. So far, there has been notable advancement in the production of high-quality films manufactured from Sn halide perovskite. Strategies involving the manipulation

of solvents, such as solvent mixing and the use of antisolvent (often chlorobenzene, CB), have shown significant potential in this area. The approach described in the report by Phuong et al. has the potential to enhance the PCE of Sn halide perovskite-based devices. In their study, they prepared thin films of the MASn($I_{1-x}Br_x)_3$ perovskite series using a solution of their precursors in a 4:1 (v:v) mixture of dimethyl formamide (DMF) and dimethyl sulfoxide (DMSO) solvent. The resulting perovskite films exhibited improved quality compared to previous methods [50,43] and identified CB as the optimal antisolvent for achieving enhanced film shape and favorable electrical characteristics. According to [41], the impact may be further improved by raising the temperature of the antisolvent. The process involves a systematic rise in the number of nucleation sites, which allows for better film coverage prior to annealing. Furthermore, the presence of a solvent may enhance the process of homogenous nucleation and provide a manageable rate of development for perovskite films [23]. This is due to the recognition that the enthalpy of crystallization is larger compared to the solvation energies of the individual ions. The crystallization process of $MASnI_3$ perovskite films may result in the creation of intermediary phases, such as $SnI_2·3DMSO$, which can lead to the production of films that are exceptionally uniform and devoid of pinholes. The intermediate regulates the pace at which the solvent evaporates and decelerates the reaction between the two halide precursors. DMSO serves to stabilize the precursors by inhibiting the development of colloidal coagulation. Additionally, it enhances the film structure by minimizing the uneven distributions of Sn and Pb [44]. Solvent-coordinated tin halide complexes, namely $[SnX_2(S)n]$ (where X represents a halide ion and S represents either DMF or DMSO), may also serve as precursors for tin halide perovskites without any impurities [41].

Solvents like DMSO and methylamine in their vapor forms may regulate the pace at which crystals develop during thermal annealing [43]. Additionally, they can also improve the stability of Sn halide perovskites under normal conditions. Sn perovskites are often treated with SnF_2 during the solution processing to prevent the oxidation of Sn^{2+} (Fujihara et al., 2017; Koh et al., 2014; W. Liao et al., 2016a; Liu, Yan, et al., 2018; Xiao et al., 2017; Y. Yu et al., 2016). SnF_2 may enhance the quality of single crystals and films by creating nucleation sites that promote crystal formation [10]. The formation of nucleation sites is achievable because SnF_2 has low solubility in perovskite precursor solvents.

3.2 Thermal Evaporation

Thermal evaporation, whether done sequentially or by co-evaporation, is recognized for producing thin films with excellent uniformity and coverage [39]. It is crucial to evaluate the appropriateness of the source materials for the deposition process since factors like material density and chemical composition have a substantial impact on the characteristics of the final film. In the case of multicomponent films like halide perovskites, where the components have varying densities, melting temperatures, and reactivity rates, a sequential deposition method may be used to accurately reproduce the stoichiometry of the source material in the film. The effectiveness of sequential thermal evaporation is maximized when the source material is formed into a stack of ultrathin layers. This enables the prompt response of the potential chemical constituents [52,53].

An example may be seen in the process and use of $CsSnBr_3$, where very thin layers of $SnBr_2$ and CsBr were successively applied [45]. Despite the enhanced thermal stability resulting from the all-inorganic composition of these Sn halide perovskites, they exhibit subpar performance as an absorber layer owing to their low Voc and significant recombination in the bulk [45,54]. One effective approach is to combine bromide ion (Br^-) with iodide ion (I^-) at the X-site to create a compound like $CsSnI_{3-x}Br_x$. This method may help reduce the development of Sn4+ and result in a broader energy bandgap and a larger open-circuit voltage (Voc). [55]cautioned that excessive increases in bandgap values should be treated with care as they may negatively impact the material's absorption characteristics, rendering it unsuitable for photovoltaic performance. The devices in the thermally evaporated hybrid form, $MASnBr_3$, with a pure Br^- X-site, as seen in the study by (Jung et al., 2016), exhibited low efficiency due to factors such as a broad bandgap of around 2.2 eV. Thermal evaporation techniques may produce high-quality films without the need for post-annealing, as shown by [39]. Despite the PCE of the device not surpassing 1.7 %, the $MASnI_3$ thin films, as they were deposited, demonstrated a well-regulated stoichiometry and enhanced morphological and electrical characteristics, all achieved without the need for the SnF_2 additive.

The inverted device structure is the most effective for photovoltaic response in tin halide perovskites, as demonstrated by many studies [38, 56–59]. Even though Sn halide perovskite-based solar cells have shown lower performance compared to their Pb halide perovskite-based counterparts, it is possible to achieve high-quality films with reduced charge recombination and minimal hysteresis by carefully controlling the film deposition conditions and using an inverted device architecture.

4. BASIC PROPERTIES OF TIN-BASED PEROVSKITES

Sn, which belongs to the same IVA group as Pb, is a very promising metal for replacing poisonous Pb in perovskites. Theoretical calculations suggest that tin-based perovskites with the formula $ASnX_3$ (where A can be MA, FA, or Cs, and X represents a halide) exhibit promising optoelectronic characteristics, such as high carrier mobility, efficient light absorption, and direct bandgaps. These properties make them suitable for applications in solar cells and other optoelectronic devices [56,60,61]. Tin-based perovskites have lately gained significant interest primarily because of their possible use in lead-free PSCs. According to reports, $MASnI_3$ has an optical bandgap ranging from 1.2 to 1.4 eV, as stated by [23,32]. This wider bandgap allows for a greater range of light absorption compared to the $MAPbI_3$ counterpart, as seen in [62] used fluorescence quenching studies to determine the carrier diffusion length in a $MASnI_3$ film, which can reach up to 500 nm. [63]made the first report on complete lead-free PSCs using $MASnI_3$ as the foundation material [22]. The researchers used a conventional and typical framework using mesoporous TiO_2 as a support structure, resulting in a PCE of 6.40 %. FA^+ is a well-studied organic cation in tin-based perovskites, similar to lead perovskites. $FAPbI_3$ exhibits numerous phases, including a yellow d phase and a dark a phase. In contrast, $FASnI_3$ has just one stable phase, which is black and has a cubic structure [21, 64]. In addition, because of the significant increase in the size of the positively charged ion in FA, $FASnI_3$ exhibits a wider bandgap compared to $MASnI_3$ [65]. In 2015, Koh et al. used $FASnI_3$ as a light-absorbing layer in PSCs, resulting in a significant current density of 24.45 mA cm^2. This achievement was attributed to the effective absorption of a wide range of light, spanning from the ultraviolet to the infrared area[66]. In recent times, a significant amount of research has been conducted on the compound $CsSnI_3$, which is a lead-free material composed entirely of inorganic elements [67,68]. $CsSnI_3$ typically exists in two different forms at room temperature. One form is known as the yellow phase (Y) and has a 1-D double-chain structure. The other form is referred to as black (B-g) and has a 3D perovskite structure. Heating the Y phase over 425 K in an inert atmosphere causes it to transform into the black cubic phase (B-a)[69,70]. As the temperature decreases, the black cubic perovskite phase (B-a) undergoes a gradual transformation into the black tetragonal phase (B-b) at 426 K and the black orthorhombic phase (B-g) at 351 K. Additionally, the B-g CsSnI3 phase undergoes oxidation to Cs2SnI6 when exposed to air[71]. The $CsSnI_3$ compound in its black B-g phase has a direct bandgap of B1.3 eV, as reported by [72, 73]. Additionally, it exhibits significant carrier mobilities, as stated by [74]. These characteristics make it a very promising material for use in solar cells. Mathews et al. observed that CsSnI3 has the potential to be used as an absorber in PSCs.

5. DEVICE STRUCTURE OF TIN-BASED PEROVSKITE SOLAR CELLS

5.1 Device Structure

PSCs are typically fabricated using two types of device structures: the normal structure and the inverted structure. These structures primarily comprise a transparent electrode composed of a transparent conductive oxide (TCO) such as indium tin oxide (ITO) or fluorine-doped tin oxide (FTO), a perovskite layer, an electron transport material (ETM), and a hole transport material (HTM) [75]. The typical arrangement may be further categorized into mesoporous and planar structures, while the inverted arrangement is typically planar [76].

Typically, when sunlight shines on a perovskite layer, electrons in the valence band (VB) get energized and go to the conduction band (CB) while leaving behind holes in the VB. Subsequently, the electrons and holes that are produced are transported to each interface and introduced into the ETM and HTM, respectively. In this context, the CB and VB of the perovskite material must establish appropriate energy level alignments with the charge transport layers. Fig. 3 shows the working mechanism of a PSC.
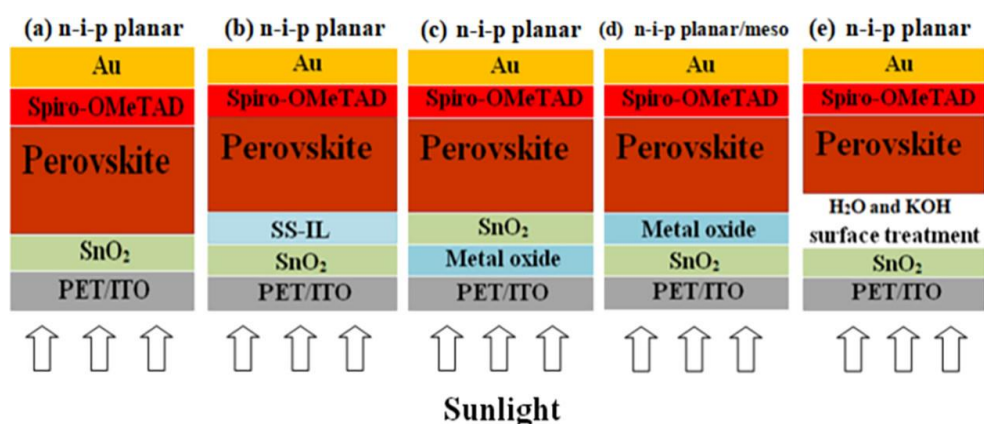
Fig. 2. Schematic diagrams of perovskite solar cells in the (a) n-i-p mesoscopic, (b) n-i-p planar, (c) p-i-n planar, and (d) p-i-n mesoscopic structures [77,78]
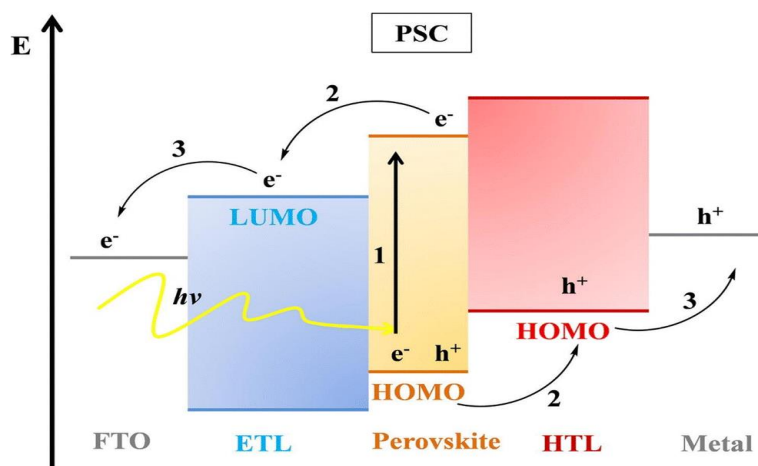

Fig. 3. The basic working mechanism of a PSC device [79]

Furthermore, it is preferable to use charge transport layers with high carrier mobilities to enable the effective movement of charges across them. Ultimately, the cathode and anode electrodes gather electrons and holes, which are then sent to external circuitry. Typical arrangement. Typically, in a regular structure, high-band-gap metal oxide semiconductors like TiO_2 and SnO_2 are used as ETMs [29, 80]. The mesoporous normal structure consists of a thin, compact layer with a mesoporous layer on top. This structure serves as both an electron transport layer (ETL) and a scaffold layer for absorbing the perovskite films [81]. The typical mesoporous structure has the benefit of being able to withstand a subpar film morphology and a limited carrier diffusion length, thereby preventing device short-circuit. This structure is often used for recently studied light absorbers [40]. Early research on tin-based PSCs used a mesoporous structure consisting of FTO/compact, TiO_2/mesoporous, TiO_2/perovskite/spiro-OMe

TAD/Au [22, 23]. For a normal planar structure, it is necessary to have a long carrier diffusion length and a good perovskite morphology [82]. In 2016, Ma and his colleagues introduced the first planar normal structure device for tin-based PSCs. The device had a structure of FTO/ blocking TiO_2/MASnI$_3$/poly(triaryl amine) (PTAA)/Au and achieved a modest PCE of 0.32% [83]. Nevertheless, conventional tin-based perovskite solar cells (PSCs) with standard configurations consistently demonstrate suboptimal efficiencies, mostly because of persistent challenges that are arduous to surmount. The addition of dopants such as lithium bis (trifluoromethanesulfonyl)imide (Li-TFSI) and 4-tert-butylpyridine (tBP) to spiro-OMeTAD to improve its hole mobility might potentially harm the underlying tin-based perovskite films [27]. Furthermore, the interaction between TiO_2 and tin-based perovskites results in the formation of Ti-O-Sn bonds, leading to the recombination of charge carriers. In response to

the drawbacks of conventional structures, researchers have pursued the development of an inverted structure. This alternative design offers benefits such as cost-effectiveness, easy manufacturing, and reduced hysteresis[84]. Wang and colleagues were the first to document the use of inverted planar $CsSnI_3$ solar cells. These cells had a structure of $ITO/NiO_x/CsSnI_3/PCBM/Al$ and had a very favorable PCE of 3.31 %. This PCE was much greater compared to solar cells with a normal structure, as reported by [74,51] reported the development of planar inverted $FASnI_3$ solar cells. These cells had a specific architecture consisting of ITO/poly (3,4-ethylenedioxythiophene) polystyrene sulfonate (PEDOT: PSS)/$FASnI_3$/ C60/ bathocuproine (BCP)/Ag. The solar cells achieved a high PCE of 6.22 %. The energy level alignment at the interfaces between the perovskite and charge transport layers has a significant impact on the performance of the device. Liu and colleagues used polyethylene glycol (PEG) to adjust the work function of PEDOT: PSS, resulting in a reduction of.1 to 4.79 eV [84]. The efficiency was enhanced from 2.01 to 5.12 % by taking advantage of the improved energy level alignment between FASnI3 and the HTM. The current maximum recorded PCE for tin-based PSCs is achieved using an inverted structure, as reported by [85].

5.2 Charge Transport Materials

In addition to the perovskite layer, the performance of PSCs is significantly affected by the physical characteristics of the charge transport materials, such as the ETMs and HTMs, as shown in Fig. 4.

In contrast to lead-based perovskites, tin-based perovskites display significant variance in their CB and VB, resulting in an unavoidable mismatch in energy alignment and a substantial loss of voltage in the V_{OC}. Therefore, it is essential to improve the energy band alignment of the devices to maximize their performance. Electronically Transmitted Mail. The ETM plays a crucial function in high-performance PSCs since it is responsible for both transporting photo-generated electrons and reducing interfacial charge recombination. Yokoyama and his colleagues [87] used niobium oxide (Nb_2O_5) as the electron transport material (ETM) in $FASnI_3$ PSCs with a flat normal structure to reduce the difference in energy levels between the conduction bands. The conduction band offset

between Nb_2O_5 and $FASnI_3$ is almost negligible, which leads to an enhanced V_{OC} from 0.27 to 0.42 V when compared to TiO_2. Fullerene and its derivatives are often used as ETMs in inverted PSCs. Lee et al. conducted a comparison between fullerene (C_{60}), phenyl-C61-butyric acid methyl ester (PCBM), and indene-C_{60} bisadduct (ICBA) as ETMs for $FA0.9PEA0.1SnI_3$ solar cells [88]. ICBA exhibits the greatest energy level for the lowest unoccupied molecular orbital (LUMO) compared to the other compounds. This results in a reduced energy difference with the CB of the $FA0.9PEA0.1SnI_3$ perovskite. As a result, the PSCs using the ICBA ETM showed a significantly greater V_{OC} of 0.651 V compared to those using PCBM and C_{60} as the ETMs, which had V_{OC}s that were 0.161 and 0.248 V lower, respectively. HTML. Due to the potential decomposition of tin-based perovskites by the dopants of spiro-OMeTAD, multiple research groups have used many alternative HTMs in tin-based PSCs in recent times. As an example, Ke and colleagues synthesized a tiny molecule called tetrakis-triphenylamine (TPE) to serve as HTM without the need for a dopant in tin-based PSCs [27]. The champion device demonstrated a PCE of 7.23 % because of its favorable energy band alignment and exceptional hole transport capabilities.

Regarding the inverted structure, it is worth noting that the typically used PEDOT: PSS material has hygroscopic properties. This characteristic might lead to a decline in the stability of the device when exposed to air. Therefore, it is necessary to optimize the HTMs located at the bottom. As an example, Cao et al. presented copper thiocyanate (CuSCN) as a hole transport material (HTM) for $FASnI_3$ solar cells. They demonstrated that CuSCN has appropriate band alignment and produced a promising PCE of 7.34 % [89]. In a separate investigation, Liao and colleagues used NiO_x as a hole extraction layer for tin-based PSCs with low dimensions, resulting in an efficiency of 5.94 % [38]. Given the significant voltage losses often seen in tin-based PSCs, there is still a need to improve the interface characteristics between tin-based perovskites and charge transport layers. Therefore, there is a pressing demand for high-throughput methods (HTMs) that can accurately align the band structure of tin-based perovskites with a minimal number of interface states in this particular sector.
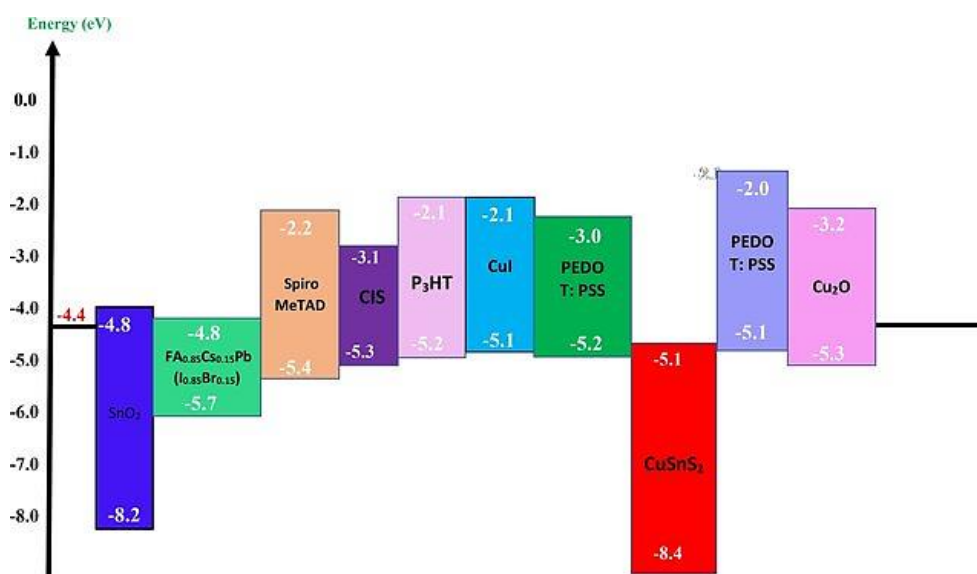
Fig. 4. Schematic representation of SnO$_2$ device arrangement with different electron and hole transport materials [77,86]

6. ENCAPSULATION TECHNOLOGY

Due to the susceptibility of Sn^{2+} to oxidation, as will be detailed later, it is crucial to promptly encapsulate tin-based PSCs to prevent oxygen contamination and enhance the long-term stability of the device. Ensuring an airtight seal around photovoltaic devices may effectively prevent the infiltration of moisture and oxygen into the perovskite layers. This approach is a viable method for improving the operational stability of the devices. The encapsulating materials should possess excellent processability, high light transmittance, and strong resistance to ultraviolet (UV) degradation and heat oxidation [90]. Perovskite layers have been encapsulated using atomic layer deposition (ALD) to improve the humidity stability of PSCs [91].

Nevertheless, the ALD technique is costly and has the potential to complicate the manufacturing process. Additional encapsulation techniques include roll lamination, where the devices are enclosed by two adhesive sheets [92]; heat sealing, which involves applying thermal energy to soften the sealants for encapsulation [80]; and the use of UV-curable epoxy to seal a piece of glass. At now, the majority of tin-based PSCs are sealed using cavity glass and UV-curable adhesives, as described by [30, 93]. However, methods for encapsulating large-area devices have not yet been established.

7. THE STABILITY OF TIN-BASED PEROVSKITES

The primary issue faced by tin-based PSCs is their inadequate resistance to air degradation. Tin-based perovskite films may undergo oxidation of Sn^{2+} to Sn^{4+}, resulting in a significant increase in p-type doping density [85]. Typically, perovskite layers that have undergone oxidation have a short duration of carrier existence and a high rate of nonradiative carrier recombination. These factors have a negative impact on the solar efficiency of PSCs. In this part, we will address the fundamental mechanism behind this problem and explore methods to improve the stability of tin-based perovskites.

8. LIMITATIONS/DRAWBACKS

Tin-based perovskites' toxicity is now the most advanced perovskites that still need the presence of Pb^{2+} to obtain exceptional optoelectronic characteristics. However, this raises concerns about the toxicity of perovskites to the environment and human health. Nevertheless, the majority of high-performance perovskites have a weight percentage of lead over 10 % [94]. Moreover, perovskites exhibit sensitivity to moisture, light, heat, and oxygen, hence raising environmental problems throughout the life cycle of perovskite photovoltaics [95]. Typically, poisonous metals include thallium, cadmium, manganese, lead, mercury, and radioactive metals. However, the

toxicity of Tin and its derivatives remains largely unexplored. However, Tin may ultimately undergo degradation and transform into an inert and water-insoluble compound known as SnO_2 when exposed to air. Therefore, the photovoltaic research community has shifted its focus to Tin as an ecologically friendly substitute for perovskites. Nevertheless, there is ongoing discussion over the relatively lower toxicity of Tin in comparison to its lead equivalents due to the intricate nature of Tin's toxicity and its environmental impacts [96]. The comparative environmental effects of Pb and Sn halide perovskites are assessed by monitoring the response of zebrafish (Danio rerio) to the breakdown byproducts of perovskites [96]. The findings suggest that zebrafish are more adversely affected by exposure to SnI_2 compared to PbI_2 because of the more severe acidification effects caused by SnI_2 as opposed to PbI_2. However, let's take into account the rapid oxidation of SnI_2 in the presence of air. The previously mentioned effect of tin-based perovskites may not be seen in situations where there is a significant focus on long-term consequences. Li et al. used plants as a means to evaluate the ecological consequences of halide perovskites. The bioavailability of heavy metals in the soil is assessed by measuring the capacity of mint plants (Mentha spicata) to absorb these metals, which serves as an indicator of metal pollution. When 250 mg kg^{-1} of perovskite was added, which is the permissible limit set by agricultural regulations in China [97], the majority of mint plants exhibited blackening and decaying, indicating lead poisoning. Upon the addition of 35 mg kg^{-1} metals, the plant roots exhibit a much lower uptake of Tin compared to lead. Perovskite's Sn^{2+} is an environmentally fragile product that may break down into Sn^{4+} molecules with limited solubility in water, resulting in reduced bioavailability. Alternatively, if the soil is contaminated just with PbI_2 or SnI_2, the concentration of metal in the roots of mint is somewhat lower compared to mint growing with soil poisoned with perovskite. The decomposition of perovskites and the bioavailability of metals are influenced by the hygroscopic character of organic cations, which in turn affects the pH of the soil. All-inorganic tin-based perovskites, such as $CsSnI_3$, have the potential to decrease the harmful impact by having lower solubility. Research on the toxicity of perovskites, particularly tin-based perovskites, is currently restricted. It is crucial to promptly develop a standardized system of biological studies to evaluate their toxicity accurately.

9. CONCLUSION

Lead perovskites have been used in the design of solar cells; however, they are known to cause adverse effects due to their toxic nature to the environment. Tin is being used as an alternative since it is readily available but also belongs to the same group as lead. It is worth noting that the synthesis techniques for these solar cells are either by solution method or thermal evaporation. It is further observed that the overall performance is influenced by the charge transport materials, which are either due to the Electron transport material (ETM) or hole transport material (HTM). This review also introduces the encapsulation methods of the PSC as a means to reduce aerial oxidation but also to improve the thermal stability of the solar cell. In brief, this review summarizes the Sn-based perovskites solar cells and how their efficiency can be modified based on the preparation method, use of either the solvent or the anti-solvent, charge transport materials, and encapsulation technology to improve PSC performance.

DISCLAIMER (ARTIFICIAL INTELLIGENCE)

Author(s) hereby declare that NO generative AI technologies such as Large Language Models (ChatGPT, COPILOT, etc.) and text-to-image generators have been used during the writing or editing of this manuscript.

ACKNOWLEDGEMENT

COMPETING INTERESTS

Authors have declared that no competing interests exist.

REFERENCES

1. Arum CT, Bbumba S, Kigozi M, Karume I, Kato M, Nsamba HK, Kiganda I, Ntale M. Synthesis of Novel Perovskite-organic Hybrid Materials for High-efficiency Photovoltaic Devices. Asian Journal of Applied Chemistry Research. 2024;15:94–106.
2. Bbumba S, Karume I, Kigozi M, Oyege I, Ntale M. How components of dye-sensitized solar cells contribute to efficient

solar energy Capture. Asian Journal of Applied Chemistry Research. 2024;15:24–40.

3. Seo J, Song T, Rasool S, Park S, Kim JY. An overview of lead, Tin, and mixed tin–lead-based abi3 perovskite solar cells. Advanced Energy and Sustainability Research. 2023;4:2200160.

4. Green MA. The path to 25% silicon solar cell efficiency: History of silicon cell evolution. Progress in photovoltaics: Research and Applications. 2009;17:183–189.

5. Green M, Dunlop E, Hohl-Ebinger J, Yoshita M, Kopidakis N, Hao X. Solar cell efficiency tables (version 57). Progress in photovoltaics: Research and Applications. 2021;29:3–15.

6. Kojima A, Teshima K, Shirai Y, Miyasaka T. Organometal halide perovskites as visible-light sensitizers for photovoltaic cells. J Am Chem Soc. 2009;131:6050–6051

7. Jeon NJ, Noh JH, Yang WS, Kim YC, Ryu S, Seo J, Seok S. Il: Compositional engineering of perovskite materials for high-performance solar cells. Nature. 2015;517:476–480.

8. Swarnkar A, Marshall AR, Sanehira EM, Chernomordik BD, Moore DT, Christians JA, Chakrabarti T, Luther JM. Quantum dot–induced phase stabilization of α-CsPbI3 perovskite for high-efficiency photovoltaics. Science (1979). 2016;354: 92–95.

9. Lim J, Kober-Czerny M, Lin YH, Ball JM, Sakai N, Duijnstee EA, Hong MJ, Labram JG, Wenger B, Snaith HJ. Long-range charge carrier mobility in metal halide perovskite thin-films and single crystals via transient Photo Conductivity. Nat Commun. 2022;13:4201

10. Xiao Z, Kerner RA, Zhao L, Tran NL, Lee KM, Koh TW, Scholes GD, Rand BP. Efficient perovskite light-emitting diodes featuring nanometre-sized crystallites. Nat Photonics. 2017;11:108–115.

11. Bu T, Li J, Li H, Tian C, Su J, Tong G, Ono LK, Wang C, Lin Z, Chai N. Lead halide–templated crystallization of methylamine-free perovskite for efficient photovoltaic modules. Science (1979). 2021;372:1327–1332

12. Lee MM, Teuscher J, Miyasaka T, Murakami TN, Snaith HJ. Efficient hybrid solar cells based on meso-superstructured organometal halide perovskites. Science (1979). 2012;338:643–647

13. Kim JY, Lee JW, Jung HS, Shin H, Park NG. High-efficiency perovskite solar cells. Chem Rev. 2020;120:7867–7918

14. Akkerman QA, Manna L. What defines a halide perovskite? ACS Energy Lett. 2020;5:604–610.

15. Akkerman QA, Rainò G, Kovalenko MV, Manna L. Genesis, challenges and opportunities for colloidal lead halide perovskite nanocrystals. Nat Mater. 2018; 17:394–405

16. Hoke ET, Slotcavage DJ, Dohner ER, Bowring AR, Karunadasa HI, McGehee MD. Reversible photo-induced trap formation in mixed-halide hybrid perovskites for photovoltaics. Chem Sci. 2015;6:613–617.

17. Knight AJ, Borchert J, Oliver RDJ, Patel JB, Radaelli PG, Snaith HJ, Johnston MB, Herz LM. Halide segregation in mixed-halide perovskites: Influence of A-site cations. ACS Energy Lett. 2021;6:799–808

18. Susic I, Gil-Escrig L, Palazon F, Sessolo M, Bolink HJ. Quadruple-cation wide-bandgap perovskite solar cells with enhanced thermal stability enabled by vacuum deposition. ACS Energy Lett. 2022;7:1355–1363.

19. Mahmud MA, Pham HT, Duong T, Yin Y, Peng J, Wu Y, Liang W, Li L, Kumar A, Shen H. Combined bulk and surface passivation in dimensionally engineered 2D-3D perovskite films via chlorine diffusion. Adv Funct Mater. 2021;31: 2104251.

20. Conings B, Drijkoningen J, Gauquelin N, Babayigit A, D'Haen J, D'Olieslaeger L, Ethirajan A, Verbeeck J, Manca J, Mosconi E. Intrinsic thermal instability of methylammonium lead trihalide perovskite. Adv Energy Mater. 2015;5:1500477.

21. Zeng C, Ramos-Ruiz A, Field JA, Sierra-Alvarez R. Cadmium telluride (CdTe) and cadmium selenide (CdSe) leaching behavior and surface chemistry in response to pH and O2. J Environ Manage. 2015;154:78–85.

22. Noel NK, Stranks SD, Abate A, Wehrenfennig C, Guarnera S, Haghighirad AA, Sadhanala A, Eperon GE, Pathak SK, Johnston MB. Lead-free organic–inorganic tin halide perovskites for photovoltaic applications. Energy Environ Sci. 2014; 7:3061–3068.

23. Hao F, Stoumpos CC, Cao DH, Chang RPH, Kanatzidis MG. Lead-free solid-state

organic–inorganic halide perovskite solar cells. Nat Photonics. 2014;8:489–494

24. Jiang X, Li H, Zhou Q, Wei Q, Wei M, Jiang L, Wang Z, Peng Z, Wang F, Zang Z. One-step synthesis of SnI2 (DMSO) x adducts for high-performance tin perovskite solar cells. J Am Chem Soc. 2021;143:10970–10976.

25. Li M, Li F, Gong J, Zhang T, Gao F, Zhang WH, Liu M. Advances in Tin (II)-based perovskite solar cells: From material physics to device performance. Small Struct. 2022;3:2100102.

26. Yu B, Chen Z, Zhu Y, Wang Y, Han B, Chen G, Zhang X, Du Z, He Z. Heterogeneous 2D/3D tin-halides perovskite solar cells with certified conversion efficiency breaking 14%. Advanced Materials. 2021;33:2102055

27. Ke W, Stoumpos CC, Spanopoulos I, Mao L, Chen M, Wasielewski MR, Kanatzidis MG. Efficient lead-free solar cells based on hollow {en} MASnI3 perovskites. J Am Chem Soc. 2017;139:14800–14806.

28. Ke W, Xiao C, Wang C, Saparov B, Duan HS, Zhao D, Xiao Z, Schulz P, Harvey SP, Liao W. Employing lead thiocyanate additive to reduce the hysteresis and boost the fill factor of planar perovskite solar cells. Advanced Materials. 2016;28.

29. Ke W, Stoumpos CC, Logsdon JL, Wasielewski MR, Yan Y, Fang G, Kanatzidis MG. TiO2–ZnS cascade electron transport layer for efficient formamidinium tin iodide perovskite solar cells. J Am Chem Soc. 2016;138:14998–15003.

30. Jokar E, Chien C, Tsai C, Fathi A, Diau EW.Robust tin-based perovskite solar cells with hybrid organic cations to attain efficiency approaching 10%. Advanced Materials. 2019;31:1804835.

31. Wang K, Liang Z, Wang X, Cui X. Lead replacement in CH3NH3PbI3 perovskites. Adv Electron Mater. 2015;1:1500089.

32. Stoumpos CC, Malliakas CD, Kanatzidis MG. Semiconducting tin and lead iodide perovskites with organic cations: Phase transitions, high mobilities, and near-infrared photoluminescent properties. Inorg Chem. 2013;52:9019–9038.

33. Kagan CR, Mitzi DB, Dimitrakopoulos CD. Organic-inorganic hybrid materials as semiconducting channels in thin-film field-effect transistors. Science. 1979;286:945–947 (1999)

34. Mitzi DB, Dimitrakopoulos CD, Kosbar LL. Structurally tailored organic− inorganic perovskites: Optical properties and solution-processed channel materials for thin-film transistors. Chemistry of Materials. 2001;13:3728–3740.

35. Chen Z, Wang JJ, Ren Y, Yu C, Shum K. Schottky solar cells based on CsSnI3 thin-films. Appl Phys Lett. 2012;101.

36. Shao S, Liu J, Portale G, Fang H, Blake GR, Ten Brink GH, Koster LJA, Loi MA. Highly reproducible Sn-based hybrid perovskite solar cells with 9% efficiency. Adv Energy Mater. 2018;8:1702019.

37. Liao Y, Liu H, Zhou W, Yang D, Shang Y, Shi Z, Li B, Jiang X, Zhang L, Quan LN. Highly oriented low-dimensional tin halide perovskites with enhanced stability and photovoltaic performance. J Am Chem Soc. 2017;139:6693–6699.

38. Zhao D, Yu Y, Wang C, Liao W, Shrestha N, Grice CR, Cimaroli AJ, Guan L, Ellingson RJ, Zhu K. Low-bandgap mixed tin–lead iodide perovskite absorbers with long carrier lifetimes for all-perovskite tandem solar cells. Nat Energy. 2017;2:1–7.

39. Yu Y, Zhao D, Grice CR, Meng W, Wang C, Liao W, Cimaroli AJ, Zhang H, Zhu K, Yan Y. Thermally evaporated methylammonium tin triiodide thin films for lead-free perovskite solar cell fabrication. RSC Adv. 2016;6:90248–90254.

40. Yokoyama T, Cao DH, Stoumpos CC, Song TB, Sato Y, Aramaki S, Kanatzidis MG. Overcoming short-circuit in lead-free CH3NH3SnI3 perovskite solar cells via kinetically controlled gas–solid reaction film fabrication process. J Phys Chem Lett. 2016;7:776–782.

41. Liu X, Wang Y, Xie F, Yang X, Han L. Improving the performance of inverted formamidinium tin iodide perovskite solar cells by reducing the energy-level mismatch. ACS Energy Lett. 2018;3:1116–1121.

42. Li Y, Sun W, Yan W, Ye S, Rao H, Peng H, Zhao Z, Bian Z, Liu Z, Zhou H. 50% Sn-based planar perovskite solar cell with power conversion efficiency up to 13.6%. Adv Energy Mater. 2016;6:1601353.

43. Liu X, Yan K, Tan D, Liang X, Zhang H, Huang W. Solvent engineering improves efficiency of lead-free tin-based hybrid perovskite solar cells beyond 9%. ACS Energy Lett. 2018;3:2701–2707.

44. Zhu HL, Xiao J, Mao J, Zhang H, Zhao Y, Choy WCH. Controllable Crystallization of CH3NH3Sn0. 25Pb0. 75I3 Perovskites for Hysteresis-Free Solar Cells with Efficiency Reaching 15.2%. Adv Funct Mater. 2017; 27:1605469.

45. Moghe D, Wang L, Traverse CJ, Redoute A, Sponseller M, Brown PR, Bulović V, Lunt RR. All vapor-deposited lead-free doped CsSnBr3 planar solar cells. Nano Energy. 2016;28:469–474.

46. Jung MC, Raga SR, Qi Y. Properties and solar cell applications of Pb-free perovskite films formed by vapor deposition. RSC Adv. 2016;6:2819–2825.

47. Ke W, Stoumpos CC, Kanatzidis MG. "Unleaded" perovskites: Status quo and future prospects of tin-based perovskite solar cells. Advanced Materials. 2019; 31:1803230.

48. Chen LJ, Lee CR, Chuang YJ, Wu ZH, Chen C. Synthesis and optical properties of lead-free cesium tin halide perovskite quantum rods with high-performance solar cell application. J Phys Chem Lett. 2016; 7:5028–5035.

49. Yu JC, Park JH, Lee SY, Song MH. Effect of perovskite film morphology on device performance of perovskite light-emitting diodes. Nanoscale. 2019;11:1505–1514.

50. Nguyen BP, Shin D, Jung HR, Kim J, Nguyen TTT, Yoon S, Yi Y, Jo W. Phase formation and local charge transport of lead-free CH3NH3Sn (I1− xBrx) 3 (0≤ x≤ 1) perovskite solar cells fabricated by solvent optimization. Solar Energy. 2019;186:136–144.

51. Liao W, Zhao D, Yu Y, Shrestha N, Ghimire K, Grice CR, Wang C, Xiao Y, Cimaroli AJ, Ellingson RJ. Fabrication of efficient low-bandgap perovskite solar cells by combining for mamidinium tin iodide with methylammonium lead iodide. J Am Chem Soc. 2016;138:12360–12363.

52. Koh TM, Fu K, Fang Y, Chen S, Sum TC, Mathews N, Mhaisalkar SG, Boix PP, Baikie T. Formamidinium-containing metal-halide: An alternative material for near-IR absorption perovskite solar cells. The Journal of Physical Chemistry C. 2014; 118:16458–16462.

53. Fujihara T, Terakawa S, Matsushima T, Qin C, Yahiro M, Adachi C. Fabrication of high coverage MASnI 3 perovskite films for stable, planar heterojunction solar cells. J Mater Chem C Mater. 2017;5:1121–1127.

54. Gupta S, Bendikov T, Hodes G, Cahen D. CsSnBr3, a lead-free halide perovskite for long-term solar cell application: insights on SnF2 addition. ACS Energy Lett. 2016; 1:1028–1033.

55. Sabba D, Mulmudi HK, Prabhakar RR, Krishnamoorthy T, Baikie T, Boix PP, Mhaisalkar S, Mathews N. Impact of anionic Br–substitution on open circuit voltage in lead free perovskite (CsSnI3-xBr x) solar cells. The Journal of Physical Chemistry C. 2015;119:1763–1767.

56. Liu C, Tai Q, Wang N, Tang G, Loi H, Yan F. Sn-based perovskite for highly sensitive photodetectors. Advanced Science. 2019; 6:1900751.

57. Gao F, Li C, Qin L, Zhu L, Huang X, Liu H, Liang L, Hou Y, Lou Z, Hu Y. Enhanced performance of tin halide perovskite solar cell by addition of lead thiocyanate. RSC Adv. 2018;8:14025–14030.

58. Zhang M, Lyu M, Yun JH, Noori M, Zhou X, Cooling NA, Wang Q, Yu H, Dastoor PC, Wang L. Low-temperature processed solar cells with formamidinium tin halide perovskite/fullerene heterojunctions. Nano Res. 2016;9:1570–1577.

59. Liao W, Zhao D, Yu Y, Grice CR, Wang C, Cimaroli AJ, Schulz P, Meng W, Zhu K, Xiong RG. Lead-free inverted planar formamidinium tin triiodide perovskite solar cells achieving power conversion efficiencies up to 6.22%. Advanced Materials. 2016;28.

60. Xie C, Liu C, Loi H, Yan F. Perovskite-based phototransistors and hybrid photodetectors. Adv Funct Mater. 2020;s30:1903907.

61. Xie C, You P, Liu Z, Li L, Yan F. Ultrasensitive broadband phototransistors based on perovskite/organic-semiconductor vertical heterojunctions. Light Sci Appl. 2017;6:e17023–e17023.

62. Lin Q, Armin A, Burn PL, Meredith P. Organohalide perovskites for solar energy conversion. Acc Chem Res. 2016;49:545–553.s

63. Snaith HJ, Abate A, Ball JM, Eperon GE, Leijtens T, Noel NK, Stranks SD, Wang JTW, Wojciechowski K, Zhang W. Anomalous hysteresis in perovskite solar cells. J Phys Chem Lett. 2014;5:1511–1515.

64. Binek A, Hanusch FC, Docampo P, Bein T. Stabilization of the trigonal high-temperature phase of formamidinium lead

iodide. J Phys Chem Lett. 2015;6:1249–1253.

65. Shi T, Zhang HS, Meng W, Teng Q, Liu M, Yang X, Yan Y, Yip HL, Zhao YJ. Effects of organic cations on the defect physics of tin halide perovskites. J Mater Chem A Mater. 2017;5:15124–15129

66. Koh TM, Krishnamoorthy T, Yantara N, Shi C, Leong WL, Boix PP, Grimsdale AC, Mhaisalkar SG, Mathews N. Formamidinium tin-based perovskite with low E g for photovoltaic applications. J Mater Chem A Mater. 2015;3:14996–15000.

67. Wang S, Wang S, Liu J. Life-cycle Green House gas emissions of onshore and offshore wind turbines. J Clean Prod. 2019;210:804–810.

68. Li W, Li J, Li J, Fan J, Mai Y, Wang L. Addictive-assisted construction of all-inorganic CsSnIBr 2 mesoscopic perovskite solar cells with superior thermal stability up to 473 K. J Mater Chem A Mater. 2016;4:17104–17110.

69. Kontos AG, Kaltzoglou A, Siranidi E, Palles D, Angeli GK, Arfanis MK, Psycharis V, Raptis YS, Kamitsos EI, Trikalitis PN. Structural stability, vibrational properties, and photoluminescence in CsSnI3 perovskite upon the addition of SnF2. Inorg Chem. 2017;56:84–91.

70. Chung I, Song JH, Im J, Androulakis J, Malliakas CD, Li H, Freeman AJ, Kenney JT, Kanatzidis MG. CsSnI3: Semiconductor or metal? High electrical conductivity and strong near-infrared photoluminescence from a single material. High hole mobility and phase-transitions. J Am Chem Soc. 2012;134:8579–8587.

71. Qiu X, Cao B, Yuan S, Chen X, Qiu Z, Jiang Y, Ye Q, Wang H, Zeng H, Li J. From unstable CsSnI3 to air-stable Cs2SnI6: A lead-free perovskite solar cell light absorber with bandgap of 1.48 eV and high absorption coefficient. Solar Energy Materials and Solar Cells. 2017;159:227–234

72. Yu C, Ren Y, Chen Z, Shum K. First-principles study of structural phase transitions in CsSnI3. J Appl Phys. 2013;114.

73. Shum K, Chen Z, Qureshi J, Yu C, Wang JJ, Pfenninger W, Vockic N, Midgley J, Kenney JT. Synthesis and characterization of CsSnI3 thin films. Appl Phys Lett. 2010;96.

74. Wang N, Zhou Y, Ju M, Garces HF, Ding T, Pang S, Zeng XC, Padture NP, Sun XW. Heterojunction-depleted lead-free perovskite solar cells with coarse-grained B-γ-CsSnI3 thin films. Adv Energy Mater. 2016;6:1601130.

75. Chen J, Park NG. Inorganic hole transporting materials for stable and high efficiency perovskite solar cells. The Journal of Physical Chemistry C. 2018; 122:14039–14063.

76. Meng L, You J, Guo TF, Yang Y. Recent advances in the inverted planar structure of perovskite solar cells. Acc Chem Res. 2016;49:155–165.

77. Dkhili M, Lucarelli G, De Rossi F, Taheri B, Hammedi K, Ezzaouia H, Brunetti F, Brown TM. Attributes of high-performance electron transport layers for perovskite solar cells on flexible PET versus on glass. ACS Appl Energy Mater. 2022;5:4096–4107.

78. Song TB, Yokoyama T, Aramaki S, Kanatzidis MG. Performance enhancement of lead-free tin-based perovskite solar cells with reducing atmosphere-assisted dispersible additive. ACS Energy Lett. 2017;2:897–903.

79. Marinova N, Valero S, Delgado JL. Organic and perovskite solar cells: Working principles, materials and interfaces. J Colloid Interface Sci. 2017;488:373–389.

80. Kim HS, Lee CR, Im JH, Lee KB, Moehl T, Marchioro A, Moon SJ, Humphry-Baker R, Yum JH, Moser JE. Lead iodide perovskite sensitized all-solid-state submicron thin film mesoscopic solar cell with efficiency exceeding 9%. Sci Rep. 2012;2:591.

81. You P, Li G, Tang G, Cao J, Yan F. Ultrafast laser-annealing of perovskite films for efficient perovskite solar cells. Energy Environ Sci. 2020;13:1187–1196.

82. Jiang Q, Chu Z, Wang P, Yang X, Liu H, Wang Y, Yin Z, Wu J, Zhang X, You J. Planar-structure perovskite solar cells with efficiency beyond 21%. Advanced Materials. 2017;29:1703852.

83. Ma L, Hao F, Stoumpos CC, Phelan BT, Wasielewski MR, Kanatzidis MG. Carrier diffusion lengths of over 500 nm in lead-free perovskite CH3NH3SnI3 films. J Am Chem Soc. 2016;138:14750–14755.

84. Liu T, Chen K, Hu Q, Zhu R, Gong Q. Inverted perovskite solar cells: Progresses and perspectives. Adv Energy Mater. 2016;6:1600457.

85. Tai Q, Cao J, Wang T, Yan F. Recent advances toward efficient and stable tin-based perovskite solar cells. Eco Mat. 2019;1:e12004.

86. Bhardwaj KS, Rai S, Sadanand, Lohia P, Dwivedi DK. Investigating the performance of mixed cation mixed halide-based perovskite solar cells using various hole-transport materials by numerical simulation. Opt Quantum Electron. 2021; 53:1–16.

87. Yokoyama T, Nishitani Y, Miyamoto Y, Kusumoto S, Uchida R, Matsui T, Kawano K, Sekiguchi T, Kaneko Y. Improving the open-circuit voltage of Sn-based perovskite solar cells by band alignment at the electron transport layer/perovskite layer interface. ACS Appl Mater Interfaces. 2020;12:27131–27139.

88. Lee M, Kim D, Lee YK, Koo H, Lee KT, Chung I. Indene-C60 bisadduct electron-transporting material with the high LUMO level enhances open-circuit voltage and efficiency of tin-based perovskite solar cells. ACS Appl Energy Mater. 2020;3: 5581–5588.

89. Cao J, Tai Q, You P, Tang G, Wang T, Wang N, Yan F. Enhanced performance of tin-based perovskite solar cells induced by an ammonium hypophosphite additive. J Mater Chem A Mater. 2019;7:26580–26585.

90. Uddin A, Upama MB, Yi H, Duan L. Encapsulation of organic and perovskite solar cells: A review. Coatings. 2019;9:65.

91. Koushik D, Verhees WJH, Kuang Y, Veenstra S, Zhang D, Verheijen MA, Creatore M, Schropp REI. High-efficiency humidity-stable planar perovskite solar cells based on atomic layer architecture. Energy Environ Sci. 2017;10:91–100.

92. Tanenbaum DM, Dam HF, Rösch R, Jørgensen M, Hoppe H, Krebs FC. Edge sealing for low cost stability enhancement of roll-to-roll processed flexible polymer solar cell modules. Solar Energy Materials and Solar Cells. 2012;97:157–163.

93. Meng X, Lin J, Liu X, He X, Wang Y, Noda T, Wu T, Yang X, Han L. Highly stable and efficient FASnI3-based perovskite solar cells by introducing hydrogen bonding. Advanced Materials. 2019;31:1903721.

94. Abate A. Perovskite solar cells go lead free. Joule. 2017;1:659–664.

95. Su P, Liu Y, Zhang J, Chen C, Yang B, Zhang C, Zhao X. Pb-based perovskite solar cells and the underlying pollution behind clean energy: Dynamic leaching of toxic substances from discarded perovskite solar cells. J Phys Chem Lett. 2020; 11:2812–2817

96. Babayigit A, Ethirajan A, Muller M, Conings B. Toxicity of Organometal halide perovskite solar cells. Nat Mater. 2016; 15:247–251

97. Li J, Cao HL, Jiao WB, Wang Q, Wei M, Cantone I, Lü J, Abate A. Biological impact of lead from halide perovskites reveals the risk of introducing a safe threshold. Nat Commun. 2020;11:310.